IMAGE FORMATION MODEL OF A 3-D TRANSLUCENT OBJECT OBSERVED IN LIGHT MICROSCOPY

Nicolas DEY[*]*, Alain BOUCHER and Monique THONNAT*

INRIA, BP 93, F-06902 Sophia Antipolis, France
{Nicolas.Dey, Alain.Boucher, Monique.Thonnat}@sophia.inria.fr

ABSTRACT

In this paper, we propose a complete model for the image formation of 3D microscopic translucent object. This model is essentially composed of 3 steps. The first step is the modeling of an object. We define a 3D distribution of complex indexes of refraction. The second step is based on ray tracing and simulates the light propagation inside the specimen. We compute an light intensity volume. Finally, we simulate a light microscope as a blurring model. It forms the 2D final image. This model of blur approximates the real Optical Transfer Function with 5 physical parameters describing the optical system. We show results of our complete model. The computed images are compared to real images of a microscopic glass sphere.

1. INTRODUCTION

We are interested in studying the image formation process of a 3D translucent object lit with incoherent light. We observe it with an optical microscope. Simulating the image formation process is the first step in performing the inverse problem: reconstructing the properties of a real specimen. We are working with image sequences, taken with a constant increasing step of the microscope focus through the specimen. On each image of the sequence, a region of the specimen appears clear, whereas the rest is blurred. Reconstructing the shape an opaque sphere observed with a light microscope has already been proposed by Nayar et al. [1] with a Shape From Focus method. In this case, we can easily find the clearest part because only the external surface of the opaque object is visible. The inside can not be seen and do not perturbate the image. In [2], Agard et al. propose a reconstruction algorithm applied to self luminescent microscopic objects. These objects are translucent, but observed in fluorescence. So, only a few parts of the object (the ones that have absorbated the fluorescent dye) are luminous. The light dispersion is preponderant over the refraction, so it is possible to extract the clearest parts of one image. In [3], Kagalwala et al. propose an image formation model for translucent specimens observed in Differential Interference Microscopy (DIC). Their work is interesting because we use similar way for our model: they got a model for the translucent object and simulate its image formation, using a ray tracing model. Nevertheless, they do not take the specimen absorption into account. This paper is structured as follows: we first describe the image formation problem in section 2, before presenting each part of our model in section 3, i.e. the object model and the optical system model. In section 4, we present the results of our works and compare a test object image sequence to a real set of images. In section 5, we conclude and propose some ideas as future works.

[*]The authors would like to thank Dr Jean-Denis SYLVAIN, Nice Sophia Antipolis University, and Dr Antoine MANGIN, ACRI S.A., for there precious colaborations. This work has been supported by the French PACA Region.

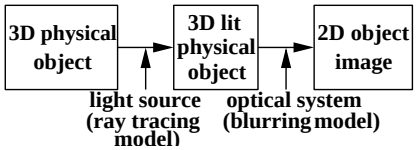

Fig. 1. Image formation model. An existing 3-D physical model is lit with an incoherent light source (this is processed with our backward ray tracing model), to obtain a 3D lit object, that can be observed with an optical system. Now observing the lit object (with our modeled microscope) gives a 2D computed image with some blur.

2. IMAGE FORMATION

With a microscope, light rays first go through the object, and then cross the optical system lenses. Our model does exactly the same by first constructing a model of the lit object, and then applying blur model on this object. Such a model takes into account 3 important steps of modeling that are represented on Fig. 1. The first one is the modeling of the real 3D physical object, without any light source. The second step is the same object, but this time lit with an incoherent light. At this level, physical phenomena of refraction and absorption occurs to build a 3D repartition of light intensity. Finally, the third step is the image construction

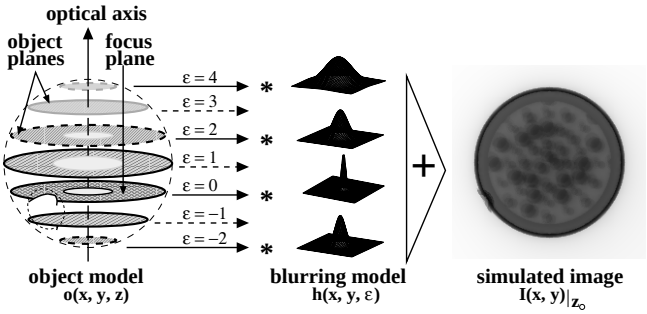

Fig. 2. To compute an image, we apply our 3-D blurring model to each object plane of the 3D lit object space: the focus defines $\varepsilon = 0$, and then, each plane is convolved with its own blurring function to give a 2D subimage. We have not represented the blurring model for all ϵ. The addition of all the subimages gives the simulated image.

of this lit space, when introducing an optical system. The 3D physical object does exist without any light source. It is defined by its own physical parameters such as, for instance, size, shape, complex refractive index, etc... The complex refractive index [4] takes the refractive index (that deviates light rays) and the absorption coefficient (that decreases light intensity) into account. Its expression is given by $\widehat{n} = n\,(1 + i\,\kappa)$ where i denotes the imaginary part. κ is called the attenuation index of the medium and n the refractive index. In our model, the object is defined as a 3D distribution of complex refractive index. We assume that the light source is monochromatic with $\lambda = 0.55\,\mu m$. When the object is lit, the light wave interacts with the physical object to give a lit physical object. The refraction and absorption phenomena occur during the light propagation inside the object. The result is a 3D distribution of intensity. Now, to observe it, we need an imaging system, like an optical microscope for instance. We model it with its incoherent Optical Transfer Function (OTF) and we suppose that it has a circular aperture. We use Stokseth's model [5] which is a good and corrected approximation of the real OTF: it only needs 5 physical parameters. It is more detailed in section 3.2. The OTF corresponds to the Fourier transform of the Point Spread Function. Observing a physical scene is a projection of a 3D space (lit object space) on a 2D space (image space). Thus it must introduce a degradation of the real scene. On an image, we note that this projection induces blur, due to the finite aperture size. The finite aperture size induces a finite depth of field. The depth of field is approximatively the part of the scene which appears clear (without blur) when we observe it. It can be mathematically defined (see [6] for example) but stays a very subjective notion. The image formation model described in [7] is only used with self fluorescent objects. We adapt it to the case of a 3D translucent object. The difference with a fluorescent object is that we have much more light in our case. To explain the image formation process, it is easier to deal with the Fourier Transform of the OTF, the Point Spread Function that we will note h. Considering that the optical axis is along the Z axis, we use the following notations (see Fig. 2): an **object-plane** is the 2D plane $o(x,\,y,\,z_n)$, owning to the 3D lit object space, with z_n constant; if z_0 is the focused object-plane, the **focus** is $o(x,\,y,\,z_0)$; any other z_n plane is defocused of $\varepsilon = z_n - z_0$; a **subimage** is a blurred image of an object-plane, called $i_n(x,\,y)$; at last, the **simulated image** $I(x,y)|_{z_0}$ is the sum of all the subimages at one focus z_0. Any optical system introduces blurring effects. For a single object-plane defocused of ε, its corresponding subimage is the result of its convolution by blurring function h: $i(x,\,y) = o(x,\,y,\,z_n) * h(x,\,y,\,\varepsilon)$. Generalizing [2] [7] for a thick object under the hypothesis of translucence and incoherent incoming light, each part of this object contributes to the final image. The final image $I(x,\,y)$ is thus the addition of the subimages, due to all the object-planes of the object. We have:

$$I(x,\,y)|_{z_0} = \sum o(x,\,y,\,z_n) * h(x,\,y,\,\varepsilon) \qquad (1)$$

The blurring function h is a 3-D function, depending on the defocus value ε. The higher is ε and the larger is the blur. To compute one image (Fig. 2), first choose the focus inside the object, to fix the $\varepsilon = 0$ value. Second, convolve the defocused object-planes with their respective blurring functions to get the subimages. Finally, add all these subimages to get one final optical slice.

3. IMAGE FORMATION MODEL

In this section, we explain in more details our model, and its different parts, under the assumptions of dealing with a microscopic object, made with an homogeneous media and lit with an incoherent monochromatic light.

3.1. Lit object model

As we said in section 2, we model a physical 3D object, defined by some physical values such as shape, size, and complex refractive index. The object model consists of a 3D distribution of voxels, each containing a complex refractive index value $\widehat{n}(x, y, z)$. Once the object is modeled, we can put a light source to make the physical object luminous. We use a ray tracing method, where rays are traced from the light source to the object (backward ray tracing), to be sure to have the most accurate rendering. Note that we do not construct a 2D image (for what ray tracing is often used), but we construct a whole 3D lit space and its intensity distribution. Using Snell-Descartes laws [4], the ray tracer simulates the interactions (reflection or refraction) of an impinging light wavefront on the object. One ray has its own

intensity, and this intensity may decrease in an absorbative medium. We follow each ray, decreasing its intensity during propagation when necessary, and changing direction when it is refracted or reflected. We define our scene as a 3D volume of voxels, each containing a complex value (complex refractive index). We are dealing with an incoherent light, so intensities are additive. So when a light ray hit a voxel, we add its intensity **at this point** to the last value present in the voxel. We repeat this operation for all the rays. On Fig. 4 (a), we have represented the result of the lit object space of a modeled sphere glass.

3.2. Blurring Model

The introduction of an optical system to observe the luminous scene is perturbing the reality: it projects a 3D physical space to a 2D image space. Even in the case of a microscope, where the harder distortions are corrected, the optical system introduces blur. This blur is due to a decrease of high frequencies due to the finite size of the aperture of the instrument. We are far away from the theorical model of "pinhole" where the depth of field is infinite (everything in the scene appears focused). We model the blur through the OTF (see section 2), which is a 3D function of the spatial frequencies $(u,\, v)$ and the defocalisation ε. Thus a thick luminous object must have some parts in focus, and others out of focus. The more out of focus is an object the more it appears blurred. In Stokseth's model [5], in the case of an optical microscope, we only need 5 easy-to-obtain physical values: the optical tube length d_i, the numerical aperture NA, the magnification M, the index of the medium between the lens of the microscope and the specimen n, and the wavelength λ. Its expression is given by Eq. 2:

$$H(q,\, \varepsilon) = (1 - 1.38\,(\tfrac{q}{f_c}) + 0.0304\,(\tfrac{q}{f_c})^2 \\ +0.344\,(\tfrac{q}{f_c})^3)\; Jinc\left(4k\, w(\varepsilon)\, \left(1 - \tfrac{q}{f_c}\right)\, \tfrac{q}{f_c}\right) \qquad (2)$$

where $q = \sqrt{u^2 + v^2}$, $k = \frac{2\,\pi}{\lambda}$, $Jinc(x) = 2\,\frac{J_1(x)}{x}$ with J_1 the first order of the Bessel function. The cut-off frequency is $f_c = \frac{2\,A}{\lambda\, d_f}$ with $d_f = \frac{d_i}{M}$. $w(\varepsilon)$ is the length path error [5].Some 2D curves of this OTF are shown in Fig. 3.

4. RESULTS

In this section, modeled images are compared with real images obtained from a microscope. The test object is a glass micro-sphere with a diameter of $(38.9 \pm 0.2)\ \mu m$ inside fuschine, a pink dye. The complex refractive index of glass is taken to be $\widehat{n}_{glass} = (1.52 + i\,3.77) \pm 0.02$. For the fuschine, we have calculated a complex refractive index of $\widehat{n}_{fuschine} = (1.33 + i\,0.08) \pm 0.05$. The error on fuschine index is greater because values are estimated. For each case

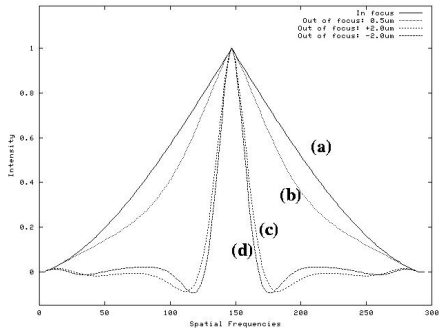

Fig. 3. We have represented some 2D curves of the OTF model. (a) in focus; (b) out of focus for $\varepsilon = 0.5\mu m$; (c) out of focus for $\varepsilon = 2.0\mu m$ and (d) for $\varepsilon = -2.0\mu m$. Please note that the OTF is not an even function of ε. This is calculated for a $60X$ / $NA\,0.80$ microscope, no immersion ($n = 1.0$), with $160mm$ of optical tube length (d_i), and lit with a mean wave length $\lambda = 0.55\mu m$.

(lit object model, computed image and real image), Fig. 4 shows one XZ view and 3 XY image views with different focus (focus shown with dashes on XZ view). The XZ sequence is taken along the optical axis, to see some consequences of the light propagation, like caustics. A caustic is a concentration of light rays with a maximum of intensities that occurs on the focal point of the translucent sphere.

Results on computed images. Fig. 4 shows some images of the computed lit object sequence (a) and of the computed image sequence (b). On the XY sequence, we can notice a small light intensity out of the object. On the XZ view, we can measure the center of the caustic, where the light intensity is the highest. From Fig. 4 (a), the distance (named x) of this point from the center of the object is approximatively $x_{computed\,object} = (87 \pm 4)\mu m$. On Fig. 4 (b), it is more difficult to evaluate because of the increasing dispersion: we estimate $x_{computed\,images} = (90 \pm 10)\mu m$. The XY images are much blurred, even the central one.

Results on real blurred images. Fig.4 (c) shows that the real caustic (XZ view) is more extended than on the computed images (a) and (b), due to camera saturation. The position of the maximum light intensity is to be near $x_{real\,images} = (78 \pm 10)\mu m$. In reality, the central XY image corresponding to a focus inside the sphere where it appears very clear, and the two others XY images are outside the sphere and blurred.

Discussion. When we compare qualitatively the real images and the computed ones, we find that our model gives very good results. The blur is increasing when focusing out from the object, like in reality. Nevertheless, the central image on the calculated image sequence is more blurred than in reality. In addition, the blur seems to be too much important. The calculated caustic on the XZ view (Fig. 4 (b)) is

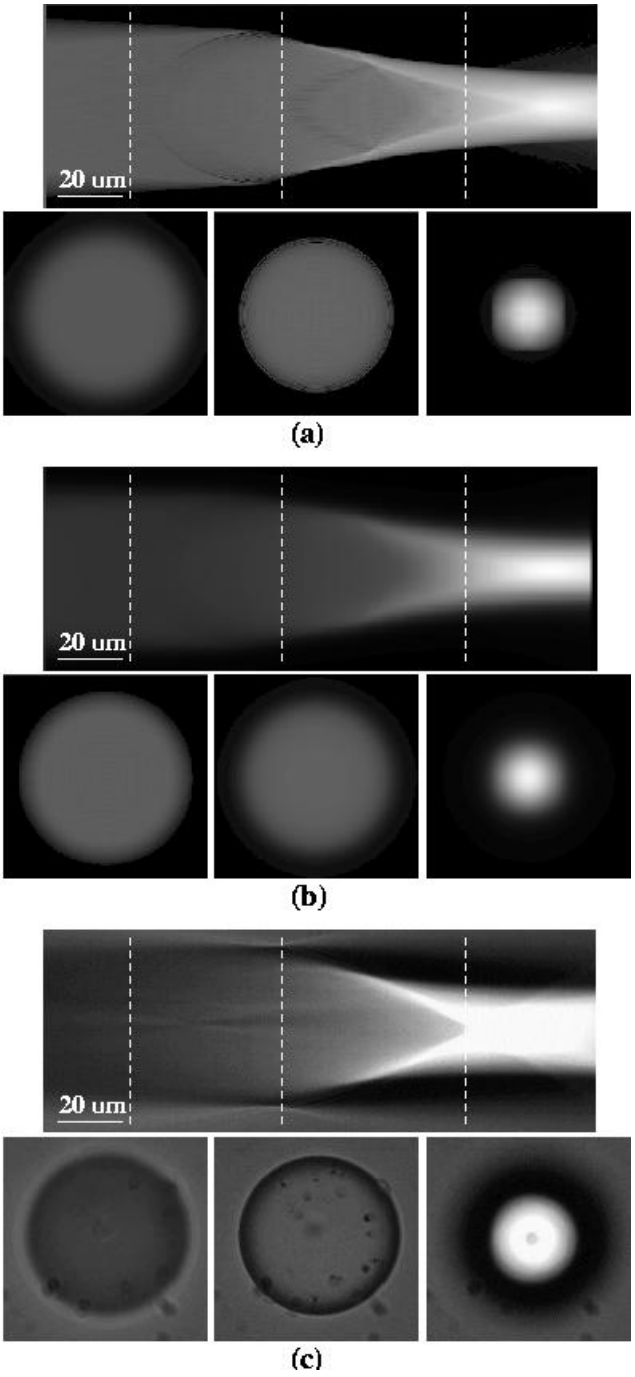

Fig. 4. The results on a real and a calculated translucent sphere. On each image (a), (b) and (c), we have represented one XZ image and 3 XY images. (a) is the calculated lit object space, (b) the corresponding calculated image sequence and (c) is the real image sequence of a translucent glass sphere.

more blurred than the real one.

5. CONCLUSION

In this paper we have presented a complete image formation model for thick microscopic translucent object. This model is essentially composed of 3 steps. The first one is the modeling of the object by defining a 3D distribution of complex indexes of refraction. Then the second one uses a ray tracing engine that simulates the travel of light rays impinging on the specimen. We compute a light intensity volume. Finally, we simulate an optical microscope that project this 3D volume onto a 2D image plan. This introduces some blur. The complete model has been tested with a 3D translucent sphere and compared to real images of 3D microscopic glass sphere with good results. The observation with the simulated optical system blurs the lit object space like in reality. Note that our model does not yet include the diffraction phenomenon; this is a scattering of light that occurs for very small objects which size are about the wavelength. As a future work, we have planed to add this phenomenon to improve the whole model. We would also like to apply this model to more complicated objects such as pollen grains, that are translucent too, and have very small details. The final goal is to link this model with some developped recognition algorithms to improve identification of 3D blurred translucent objects.

6. REFERENCES

[1] S.K. Nayar and Y. Nakagawa, "Shape from focus," *IEEE Trans. Patt. Anal. Mach. Int.*, vol. 16, no. 8, pp. 824–831, Aug. 1994.

[2] D.A. Agard, Y. Hiraoka, P. Shaw, and J.W. Sedat, "Fluorescence microscopy in three dimensions," *Methods Cell Biol.*, vol. 30, pp. 353–377, 1989.

[3] F. Kagalwala and T. Kanade, "Simulating DIC microscope images: From physical to a computational model," in *Workshop on Photometric Modelling in Computer Vision and Graphics*, IEEE Computer Society, Ed., 1999.

[4] M. Born and E. Wolf, *Principles of Optics*, Cambridge University Press, 7th (expanded) edition, 1999.

[5] P.A. Stokseth, "Proprerties of a defocused optical system," *Journal of Optic Society of America*, vol. 59, no. 10, pp. 1314–1321, Oct. 1969.

[6] C.J.R. Sheppard, "Depth of field in optical microscopy," *J. of Microscopy*, vol. 149, pp. 73–75, Jan. 1988.

[7] K.R. Castleman, *Digital Image Processing*, Prentice Hall, 1996.